

## Effect of Stress on Flow and Transport in Fractured Rock Masses Using a Modified Crack Tensor Theory

Z. Wang<sup>1,2</sup>, J. Rutqvist<sup>1</sup>, Y. Wang<sup>3</sup>, Y. Dai<sup>2,4</sup>

**Abstract:** We used a slightly modified version of Oda's crack tensor theory for developing and applying a modeling approach (that we characterize as a discrete continuum) to upscale the hydraulic and mechanical properties of fractured rock masses. The modified crack tensor theory was used to calculate the stress-dependent permeability tensor and compliance tensor for the individual grid block. By doing this, we transformed a discrete fracture network model into a grid-based continuum model. The methodology was applied to a benchmark test related to fluid flow and transport through a  $20 \times 20$  m model domain of heavily fractured media. This benchmark test is part of the international DECOVALEX project, thus providing us with the opportunity to compare our results with the results of independent models. We conducted the hydromechanical analysis with TOUGH-FLAC, a simulator based on the TOUGH2 multiphase flow code and FLAC3D geomechanical code, using a multiple interacting continua (MINC) method to simulate the flow and transport of fractured rock. The results of our simulations were consistent with the results of the other independent modeling approaches.

**Keywords:** Coupled hydro-mechanical processes, fractured rock, stress-dependent permeability, crack tensor theory

### 1 Introduction

Coupled hydromechanical effects, such as the effect of stress on permeability, could have a significant impact on flow and transport in fractured rock (Rutqvist and

---

<sup>1</sup> Earth Science Division, Lawrence Berkeley National Laboratory (LBNL), Berkeley, CA 94720 USA.

<sup>2</sup> School of Aerospace Engineering and Applied Mechanics, Tongji University, Shanghai 200092, China.

<sup>3</sup> Hohai University, Nanjing, China.

<sup>4</sup> Corresponding author. Tel.:+86 21 65983708; fax:+ 86 21 65983708. E-mail address: ydai@tongji.edu.cn

Stephansson 2003). These are complex processes that can be studied using numerical modeling, although not without raising difficulties related to upscaling and deriving representative values for both mechanical and hydrological parameters. In this study, we used a modified crack tensor theory (Oda 1986) to upscale the hydraulic and mechanical properties determined from a discrete-fracture-network model to calculate the stress-dependent permeability, which we call a discrete continuum model (Leung, Rutqvist et al. 2009), enabling us to consider the stress effect on flow and transport in fractured rock masses. With this new model, the discrete-fracture-network model was transformed into a grid-based continuum model. We implemented this approach into the framework of TOUGH-FLAC (Rutqvist, Wu et al. 2002), a simulator that links the TOUGH2 (Pruess, Oldenburg et al. 1999) multiphase fluid flow code with the FLAC3D (Itasca Consulting Group 2006) geomechanical code.

We applied this methodology to a 2D BMT (Bench Mark Test) problem denoted as Task C in the international DECOVALEX project. The BMT consists of a  $20 \times 20$  m model domain with a 2D fracture-network model (Figure 1) of 7797 individual fractures with correlated aperture length and the effects of stress and hydraulic pressure gradients are considered through various boundary conditions (Figure 2).

For the mechanical boundary conditions, a constant vertical stress of 5 MPa is specified at the top and bottom surfaces whereas a varying horizontal stress is specified for the right- and left-hand side boundaries to capture different fracture shear behaviors inside the model (Figure 2). We apply the horizontal stress at increasing magnitude, corresponding to stress ratio ( $K$ ) of horizontal/vertical stress, varying from 1,2,3,5, to progressively induce shear failure along fractures within the model.

At each set of the stress boundary conditions (after the model is in an equilibrium state), fluid flow and transport through the model is simulated by the specific hydraulic boundary conditions representing a hydraulic gradient P1-P2 (Figure 2). For such hydraulic boundary conditions, a constant pressure gradient of  $1.0 \times 10^4$  Pa/m and 10 Pa/m is simulated.

Mechanical properties of rock matrix and fractures are listed in Table 1. For simplicity, mechanical and hydraulic apertures are assumed to be equal.

## **2 Methodology**

### **2.1 Modified crack tensor theory**

The first section should be labeled Abstract; and should contain a brief description of the contents of the paper. The section of abstract should not be numbered. Subsequent sections should be numbered consecutively in Arabic numbers, starting from 1.

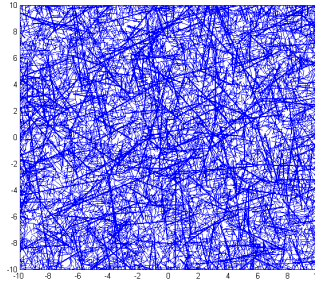


Figure 1: 2D BMT fracture network

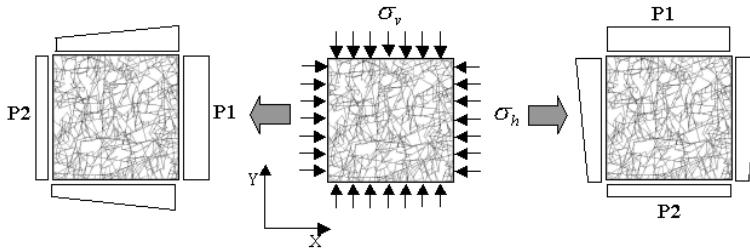


Figure 2: Mechanical and hydraulic boundary conditions

Table 1: Model properties of intact rock and fractures

Properties		value
Intact rock	Elastic modulus, $E$ (GPa)	84.6
	Poisson's ratio, $\nu$	0.24
Fractures	Shear stiffness, $K_s$ (GPa/m)	434
	Friction angle, $\phi$ ( $^\circ$ )	24.9
	Dilation angle, $d$ ( $^\circ$ )	5
	Cohesion, $c$ (MPa)	0
	Critical shear displacement for dilation, $U_{cs}$ (mm)	3
	Minimum aperture value, $a_{res}$ ( $\mu\text{m}$ )	1
Maximum aperture value, $a_{max}$ ( $\mu\text{m}$ )	200	

According to the BMT definition, the normal stiffness of a single fracture is linked to the normal stress and initial fracture aperture by (Baghbanan and Jing 2008)

$$K_n = \frac{(10\sigma_n + \sigma_{nc})^2}{9\sigma_{nc}b_0} \quad (1)$$

where  $\sigma_n$  is normal stress across the fracture,  $b_0$  is the initial aperture, and  $\sigma_{nc}$  is critical normal stress defined as  $\sigma_{nc}[\text{MPa}] = 0.487 \times b_0[\mu\text{m}] + 2.51$ .

A constant shear stiffness of  $K_s = 434$  (GPa) is used for simplicity (Table 1).

The anisotropy for the permeability and elastic stiffness was obtained using Oda's crack tensor theory, with the theory it formulated as a discrete summation of contributions from each fracture that intersect an element volume. We could apply this discrete summation approach because the description of fractures given by the Task C BMT definition is explicit (each fracture is known by its position and its geometric properties-length orientation and aperture).

The basic quantities of the crack tensor for each crack in an element are as follows:

$$F_{ij} = \frac{1}{V_e} \frac{\pi}{4} D^3 n_i n_j \quad (2)$$

$$F_{ijkl} = \frac{1}{V_e} \frac{\pi}{4} D^3 n_i n_j n_k n_l \quad (3)$$

$$P_{ij} = \frac{1}{V_e} \frac{\pi}{4} D^2 b^3 n_i n_j \quad (4)$$

where  $F_{ij}$ ,  $F_{ijkl}$ ,  $P_{ij}$  are basic crack tensors,  $V_e$  the is element volume,  $D$  is the diameter of the crack,  $b$  is the aperture of the crack, and  $\mathbf{n}$  is the unit vector of normal orientation for each crack with the component  $n_i$  ( $i=1,2,3$ ).

By using the quantities and the mechanical properties for each fracture, we calculate the anisotropic compliance tensor  $C_{ijkl}$  and permeability tensor  $k_{ij}$  using

$$C_{ijkl} = \sum^{NCR} \left[ \left( \frac{1}{K_n D} - \frac{1}{K_s D} \right) F_{ijkl} + \frac{1}{4K_s D} (\delta_{ik} F_{jl} + \delta_{jk} F_{il} + \delta_{il} F_{jk} + \delta_{jl} F_{ik}) \right] \quad (5)$$

$$k_{ij} = \sum^{NCR} \frac{1}{12} (P_{kk} \delta_{ij} - P_{ij}) \quad (6)$$

where NCR is number of cracks in an element, and  $\delta_{ij}$  is Kronecker's delta.

So the total elastic compliance tensor can be formulated as

$$T_{ijkl} = C_{ijkl} + M_{ijkl} \quad (7)$$

$$M_{ijkl} = (1/E) [(1 + \nu) \delta_{ik} \delta_{jl} - \nu \delta_{ij} \delta_{kl}] \quad (8)$$

where  $M_{ijkl}$  is the elastic compliance tensor of the intact rock.

### 2.2 Stress/aperture coupling with considering shear dilation

The stress effect on the permeability tensor was evaluated for each element considering stress-induced aperture changes for each fracture intersection of the element. Stress-induced aperture change is expressed as follows:

$$b = b_0 - \delta + \Delta b_{dil} \tag{9}$$

$$\delta = \frac{9\sigma_n b_0}{\sigma_{nc} + 10\sigma_n} \tag{10}$$

where  $\delta$  is normal closure caused by an increase in normal stress, and  $\Delta b_{dil}$  is dilatational normal displacement. Eq.(10) displays the typical nonlinear normal stress/aperture relationship for rock fractures (Baghbanan and Jing 2008).

The approach for modeling shear dilation is shown in Figure 3. If the shear stress  $\tau$  on a fracture is below the critical shear stress  $\tau_{sc}$ (Region 1), no normal displacement resulting from shear occurs. When the shear stress is larger than the critical shear stress (Region 2), slip occurs, and the fracture shear stiffness in Region 2 is calculated using Eq.(11)

$$K_{s2} = \eta \frac{G}{r} \tag{11}$$

where  $G$  is the shear modulus of the intact rock,  $r$  is the radius of the fracture, and  $\eta$  is a factor with a value that depends upon the geometry of the slip patch. In our case, we may consider a circular crack in which  $\eta = 7\pi/24$ .

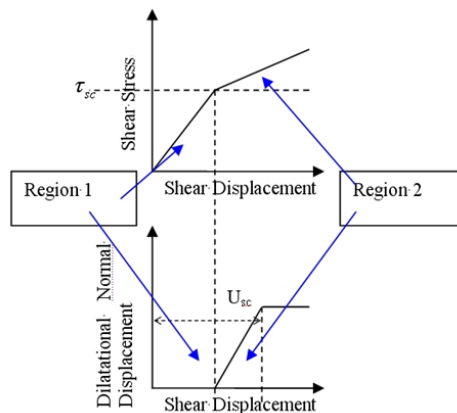


Figure 3: Strategy for modeling shear dilation

Thus, the dilatational normal displacement can be calculated using

$$\Delta b_{dil} = \frac{\tau - \tau_{sc}}{K_{s2}} \times \tan(d) \quad (12)$$

### 2.3 Calculation procedure

When the stress ratio  $K=0$ , we can use the fracture geometry information and mechanical information to calculate the initial total elastic compliance tensor and permeability tensor. When the stress ratio  $K=1$ , we first assign initial total elastic compliance tensor fields to each element in the FLAC3D model (employing a user-defined elastic anisotropic constitutive model) and calculate the new stress state. Note that because of the heterogeneous compliance within the model, with different compliance tensors for each element, the new stress state will be heterogeneous, somewhat different from the stress applied at boundaries. Then, we use the new stress fields to calculate the stress induced fracture change and update the permeability tensor fields and compliance tensor fields. With the permeability tensor defined in each element, we use TOUGH2 to simulate the flow and transport through the model. The same procedures are used for stress ratios  $K=2, 3$ , and 5. Consequently, the elastic stiffness and permeability tensors are updated anisotropically and heterogeneously, depending on the stress state when stress ratio  $K$  increases from 0 to 5. The flowchart of calculation using TOUGH-FLAC is shown in Figure 4.

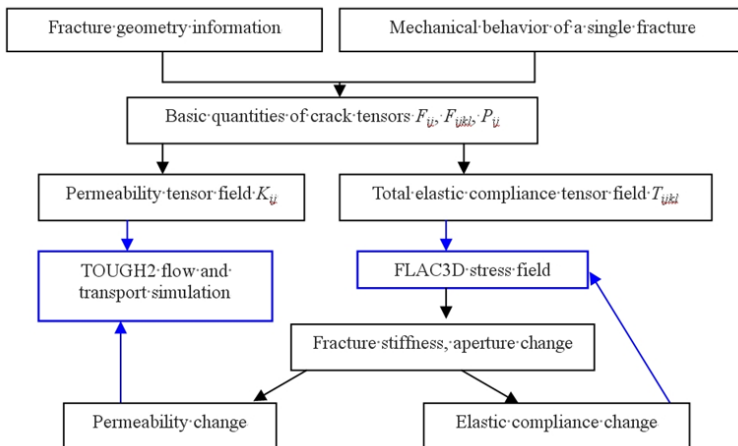


Figure 4: Flowchart of calculation

### **3 Results and discussion**

We used a “multiple interacting continua” (MINC) method (Pruess and Narasimhan 1985) in TOUGH2 to perform the flow and transport simulation, which characterizes the rock-matrix-diffusion process in the solute transport simulation. One fracture continuum and three matrix continua were used in the MINC model. In the simulations presented in this paper we divided the model domain into  $40 \times 40$  elements of side length 0.5 m. TOUGH-FLAC results (denoted as LBNL) were compared with three other teams with different approaches. The IC team used a discrete fracture network (DFN) model with computer program NAPSAC, whereas KTH used a 2D discrete element code UDEC, and TUL used a combined DFN and EC (equivalent continuum) flow and solute transport simulation code FLOW123D. Permeability tensor fields under different stress ratios from  $K=0$  to  $K=5$  are shown in Figure 5. When the stress ratio  $K$  increases, the permeability of  $K_x$  and  $K_z$  within the modeling domain decreases correspondingly. We used the flow rate at a downstream outlet to inversely calculate the equivalent permeability. Figure 6 shows the resulting equivalent modeling domain permeability changes at different stress ratios. The results in Figure 6 are consistent with Figure 5 and are sensible. For example, assuming an increasing horizontal stress while keeping a constant vertical stress, it would be expected that the equivalent vertical permeability decreases much more than the equivalent horizontal permeability.

For the transport calculation, we used a solute transport approach, which can be described as follows: (1) zero initial concentration over the entire model; (2) a short interval of constant concentration at the inlet boundary; (3) thereafter, zero concentration inflow along all the boundaries, including the lateral sides parallel to the macroscopic flow direction.

Under the high hydraulic pressure gradient of  $10^4$  Pa/m, advection is the main “driving force” of solute transport. As shown in Figure 7, under a high hydraulic gradient a negligible amount of solute diffuses into the rock matrix no matter what kind of stress state exists. The simulation results for the case of horizontal flow along a relatively high horizontal gradient are compared in terms of breakthrough curves in Figure 8. When  $K=0$  (Figure 8(a)), the breakthrough curves given by the four teams are quite similar. When considering the stress effects (Figure 8(b-d)), the four teams predicted a general shift in breakthrough curves in the longer time direction with increasing stress ratios.

The rock-matrix diffusion has an important influence on transport behavior under low hydraulic gradients (10 Pa/m) (Figure 9). The general trend of breakthrough curves shifting with increasing stress ratios was consistent with the high hydraulic gradient case. The much longer tails for breakthrough curves assuming matrix

diffusion indicate that a portion of solute could stay in the matrix micro pores for a long time before diffusing back to the fractures. Under a low hydraulic gradient, rock-matrix diffusion will retard solute transport. As shown in Figure 10, when the stress ratio increases, more solute will diffuse into the matrix, and as a result, solute transport will be strongly retarded.

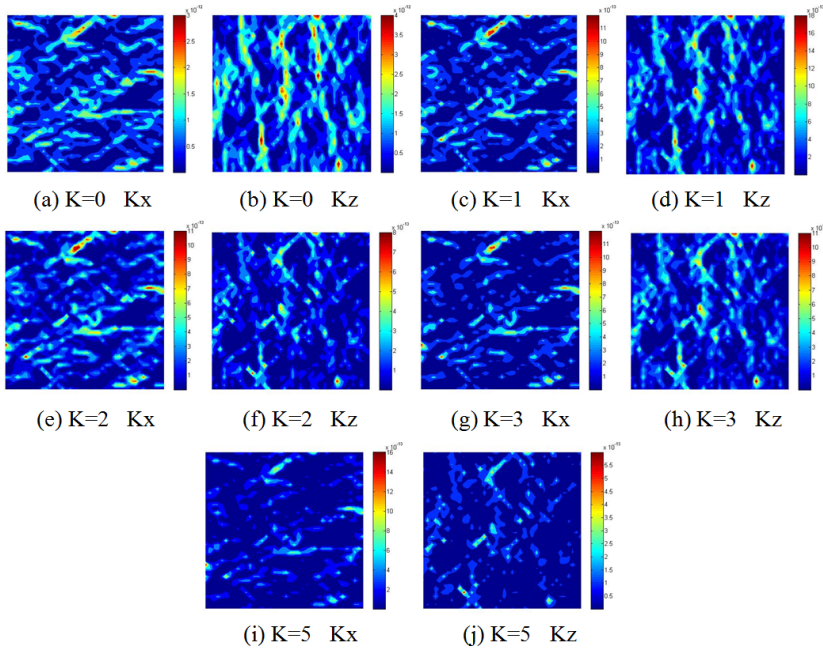


Figure 5: Permeability tensor fields with increasing stress ratio from K=0 to K=5

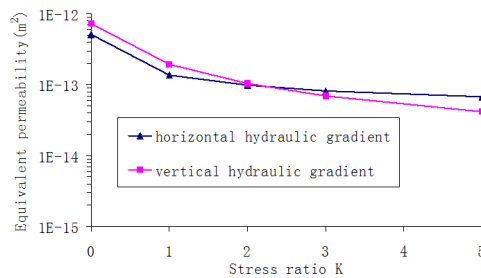


Figure 6: Equivalent permeability for horizontal and vertical flow at different stress ratios



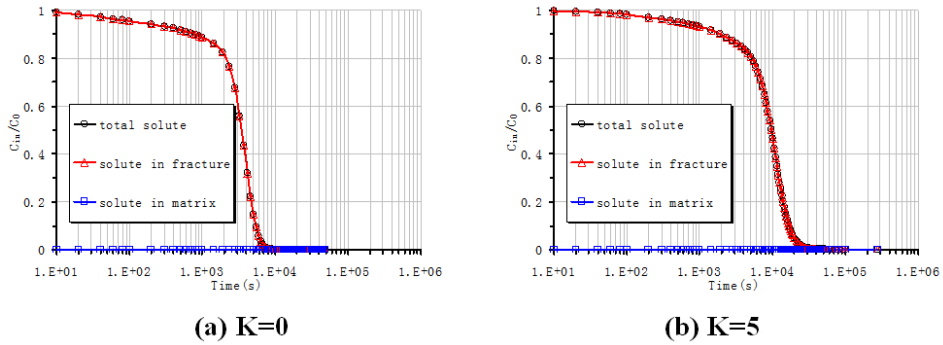


Figure 7: Solute concentration variation in fractures and rock matrix when  $K=0, 5$  under a horizontal hydraulic gradient of  $10^4$  Pa/m

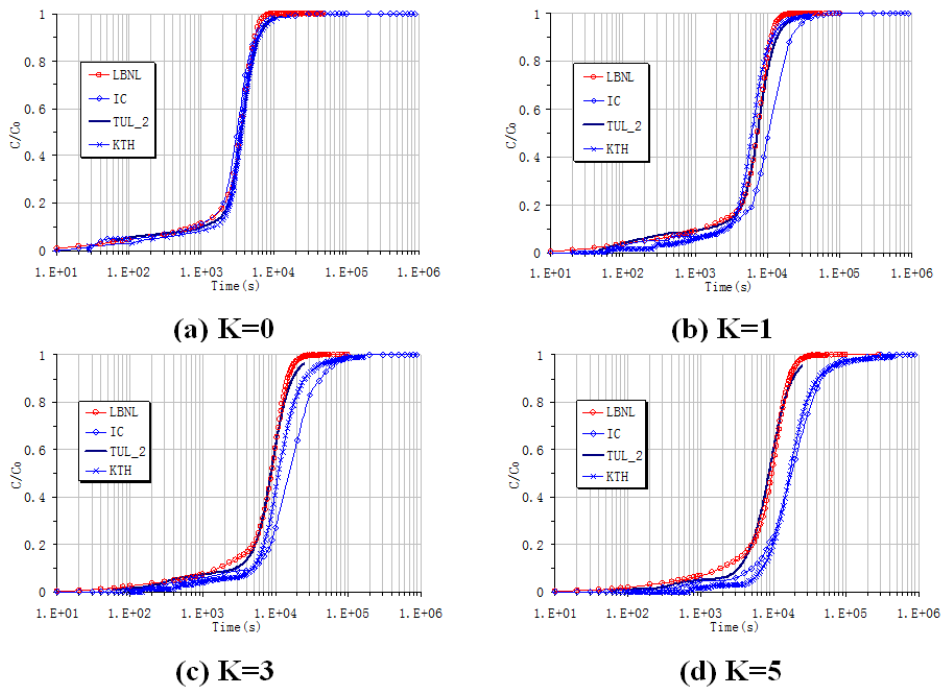


Figure 8: Comparison of breakthrough curves for conservative tracers exiting from all the three outlet boundaries with increasing stress ratio, under a horizontal hydraulic gradient of  $10^4$  Pa/m

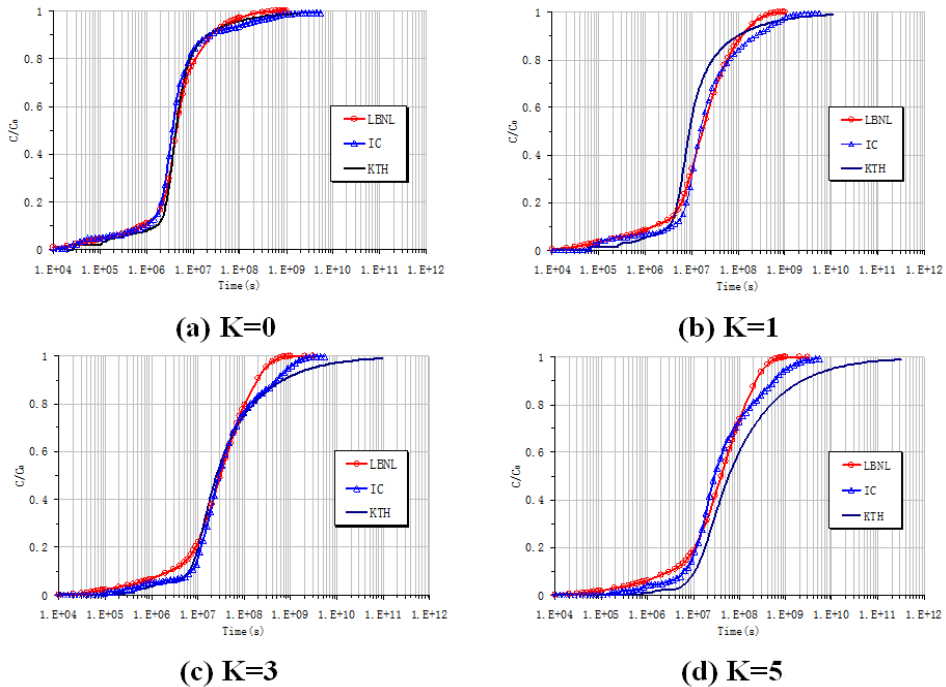


Figure 9: Comparison of breakthrough curves for interacting tracers exiting from all the three outlet boundaries with increasing stress ratio, under a horizontal hydraulic gradient of 10 Pa/m

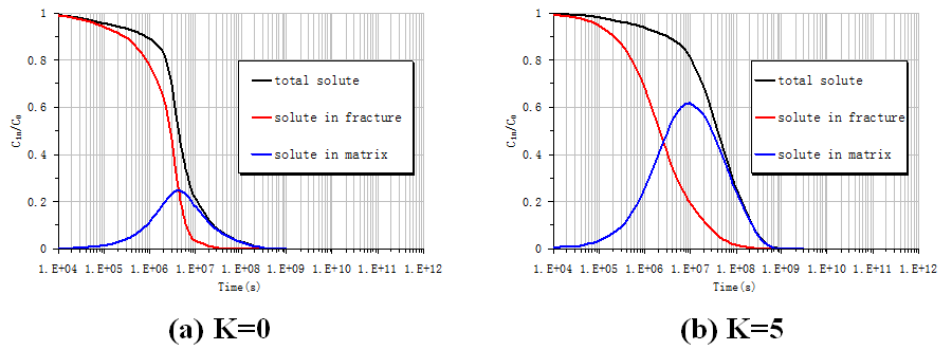


Figure 10: Solute concentration variation in fractures and rock matrix when  $K=0, 5$  under a horizontal hydraulic gradient of 10 Pa/m

#### **4 Concluding remarks**

In this paper, the stress effect on fluid flow and transport in fractured rock masses is investigated through a discrete continuum model derived from a modified crack tensor theory. We applied this methodology to a 2D benchmark test denoted as Task C in the DECOVALEX-2011 project. Results were compared with other independent model simulation results, including discrete fracture models, and the result comparisons show good agreement. Some conclusions can also be drawn:

1. When the stress ratio increases, fractures aperture close, resulting in a reduction of permeability and porosity, and solute is significantly retarded as a result of the permeability reduction.
2. When the model is under a low hydraulic gradient, rock-matrix diffusion in addition to advection will play a very important part in solute transport, retarding the solute transport substantially.

In this paper, we applied a one-way coupled hydro-mechanical model, in which we considered the stress-dependent permeability, but not pore-pressure effects on fracture deformation. The one-way coupled approach is justifiable in this case, because the fluid pressure is very small compared to the applied stress. However, our approach can be readily extended and applied for two-way coupled problems, and this possibility will be the subject of future studies.

#### **Acknowledgement**

The first author would like to acknowledge the financial supports from National Basic Research Program of China (973 Program: 2011CB013800) and China Scholarship Council (CSC). Financial support was also provided by the UK Nuclear Decommissioning Authority (NDA) to the Lawrence Berkeley National Laboratory through the National Energy Technology Laboratory, under the U.S. Department of Energy Contract No. DE-AC02-05CH11231. Editorial review by Dan Hawkes at the Berkeley Lab is greatly appreciated.

#### **References**

- Baghbanan, A.; Jing, L.** (2008): Stress effects on permeability in fractured rock masses with correlated fracture length and aperture. *International Journal of Rock Mechanics and Mining Sciences*, vol. 45, no.8, pp.1320-1334.
- Itasca Consulting Group.** (2006). *FLAC3D, Fast Lagrangian Analysis of Continua in 3 Dimensions, Version 3.1*. Minneapolis, Minnesota.
- Leung, C. T. O.; Rutqvist, J, et al.** (2009): The use of TOUGH-FLAC for coupled hydro\_mechanical modeling of fractured rock masses. *Proceedings of the Tough2*

*symposium 2009*, Lawrence Berkeley National Laboratory, Berkeley, September 14-16, 2009.

**Oda, M.** (1986): An equivalent continuum model for coupled stress and fluid flow analysis in jointed rock masses. *Water Resources Research*, vol.22, No.13, pp.1845-1856.

**Pruess, K.; Narasimhan, T. N.** (1985): A practical method for modeling fluid and heat-flow in fractured porous-media. *Society of Petroleum Engineers Journal*, vol.25, no.1, pp.14-26.

**Pruess, K. O.; Oldenburg, C. M.; Moridis, G.J.** (1999): *TOUGH2 User's Guide Version 2*. Lawrence Berkeley National Laboratory

**Rutqvist, J.; Stephansson, O.** (2003): The role of hydromechanical coupling in fractured rock engineering. *Hydrogeology Journal*, vol.11, no.1, pp.7-40.

**Rutqvist, J.; Wu, Y. S.; Tsang, C.F; Bodvarsson, G.** (2002): A modeling approach for analysis of coupled multiphase fluid flow, heat transfer, and deformation in fractured porous rock. *International Journal of Rock Mechanics and Mining Sciences*, vol.39, no.4, pp.429-442.